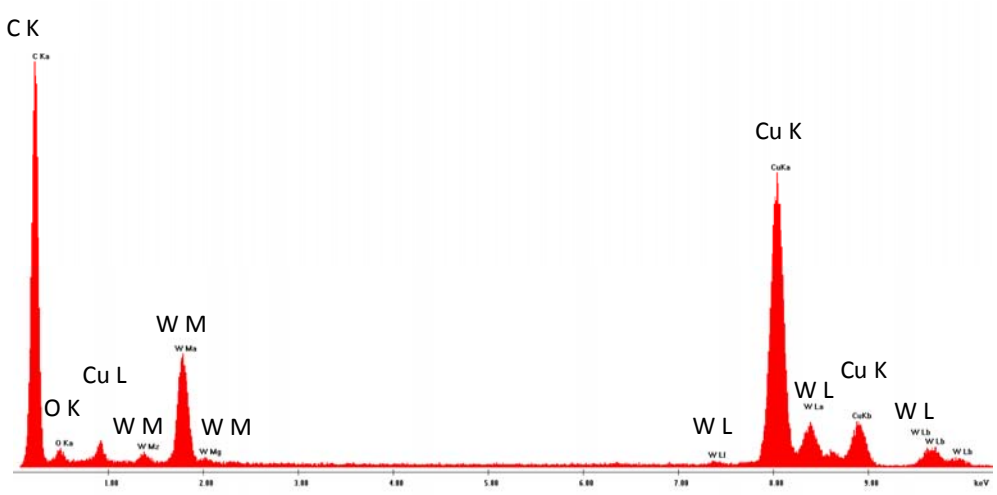

Fig. S1. EDX spectrum of the PtW_{mod}/C initial sample.

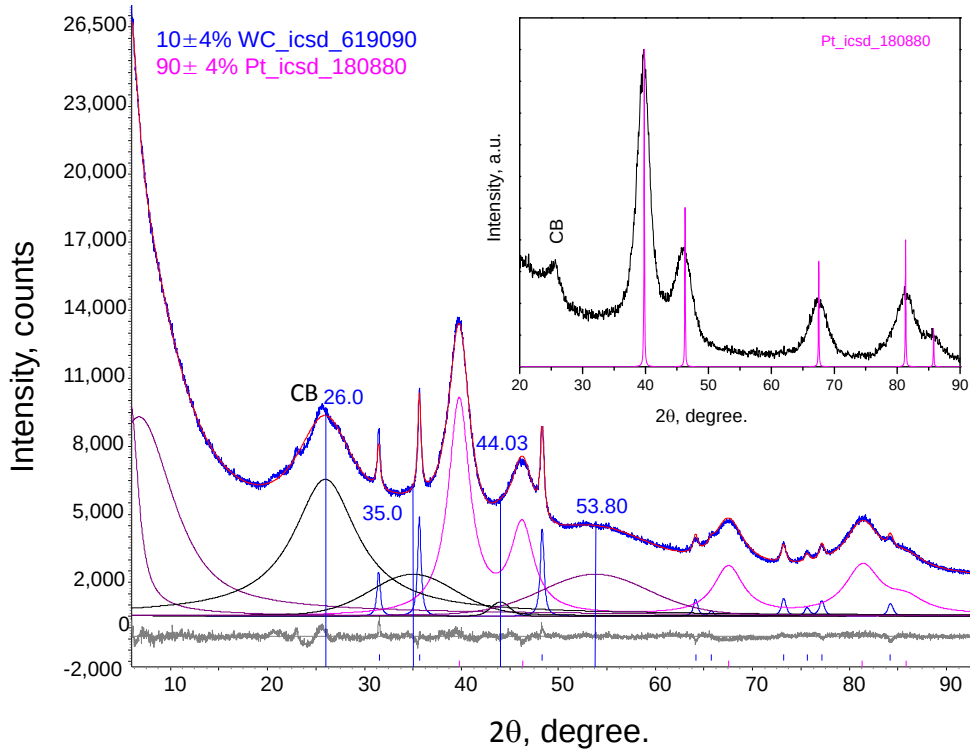

Fig. S2. XRD pattern of the initial samples: the modified PtW_xC/C and the Pt/C (inset), respectively.

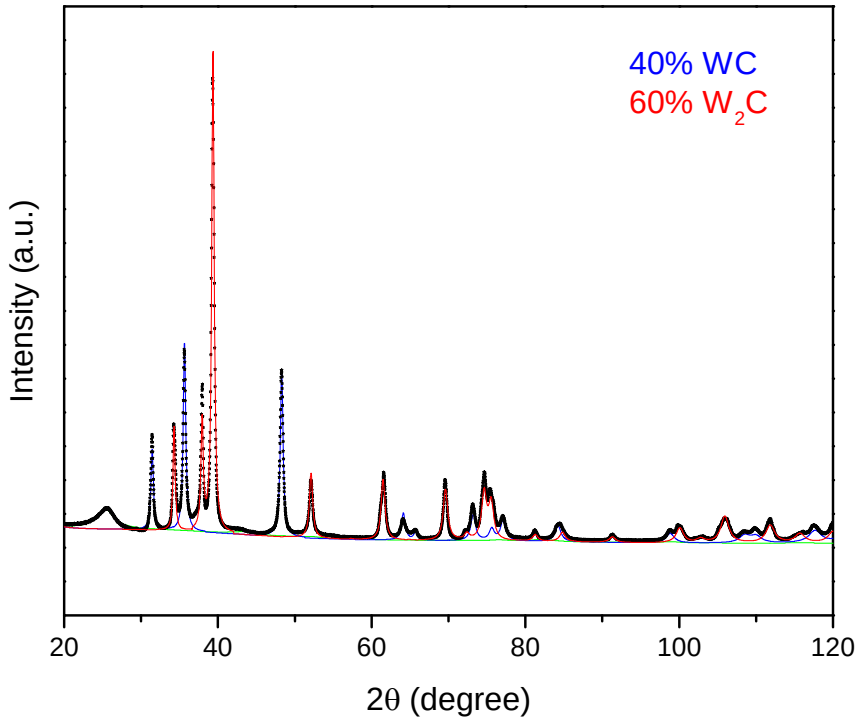

Fig. S3. XRD pattern of the Pt-free modified sample WxC/C.

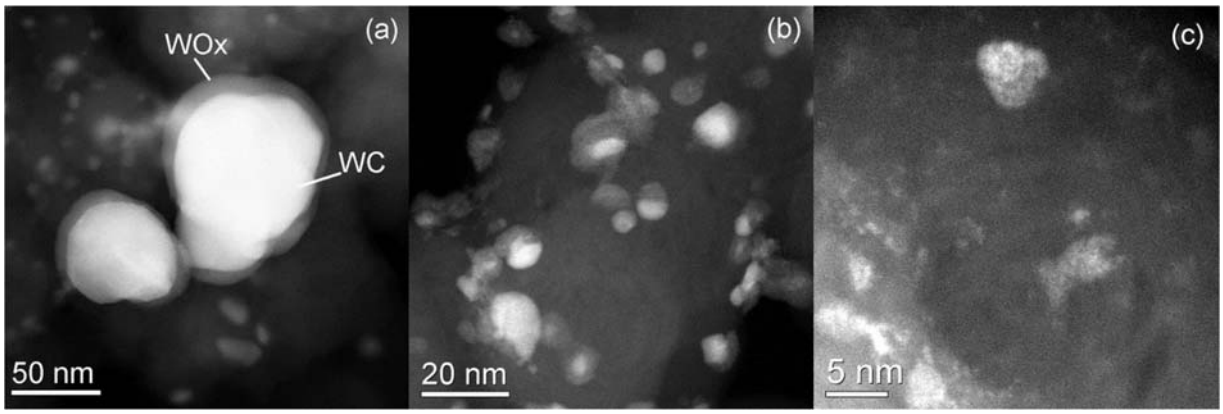

Fig. S4. HAADF STEM micrographs which show the core (WC)-shell (WOx) structure of the WxC submicron particles and WxC clusters.

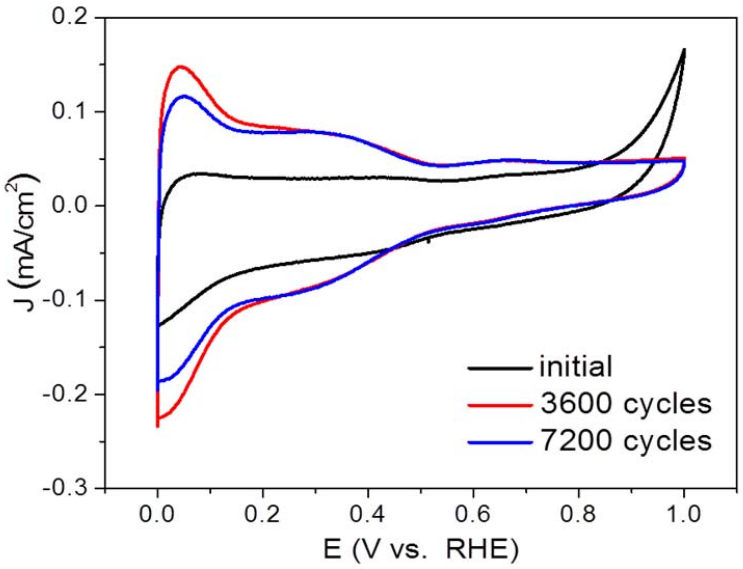

Figure S5. Cyclic voltammetry profile of the Pt-free W_xC/C sample.

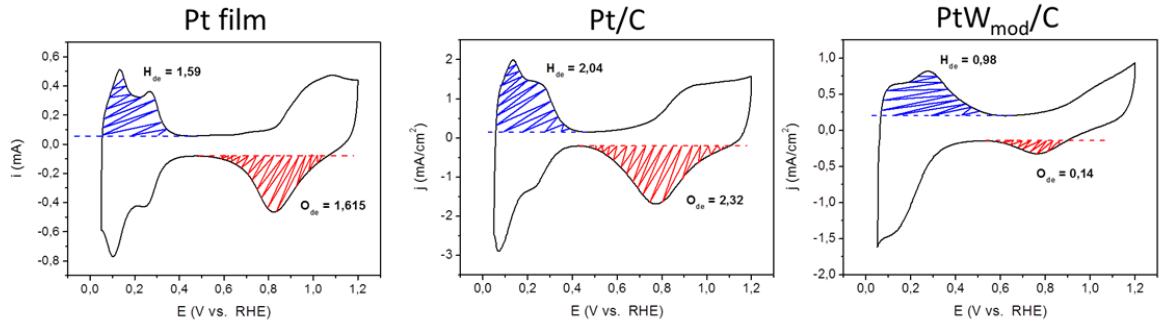

Figure S6. Cyclic voltammetry profiles of the Pt film, the Pt/C and the PtW_{mod}/C samples. One can see that the ratio of the H_{de} to the O_{de} areas in the case of the Pt film and the Pt/C sample is close to 1 compared to the modified PtW_{mod}/C sample with the ratio value of 7. The comparable values of H_{de} and the O_{de} areas in the case of only Pt containing samples justifies the use of the O_{de} area for ECSA loss calculations in order to distinguish contributions of Pt and W for the modified sample.

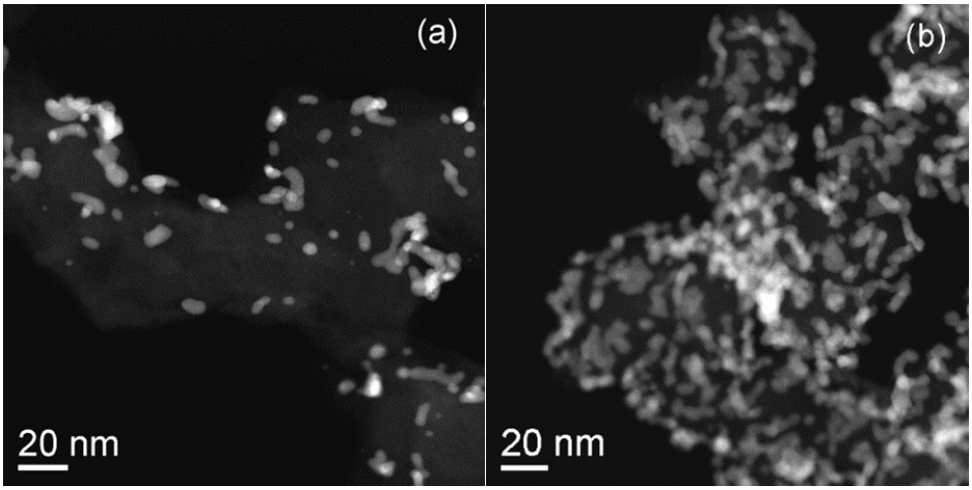

Fig. S7. HAADF STEM images of the common regions consisting of small carbon particles after electrochemical corrosion. a) PtC; b) –PtW_xC_{mod}/C, respectively.

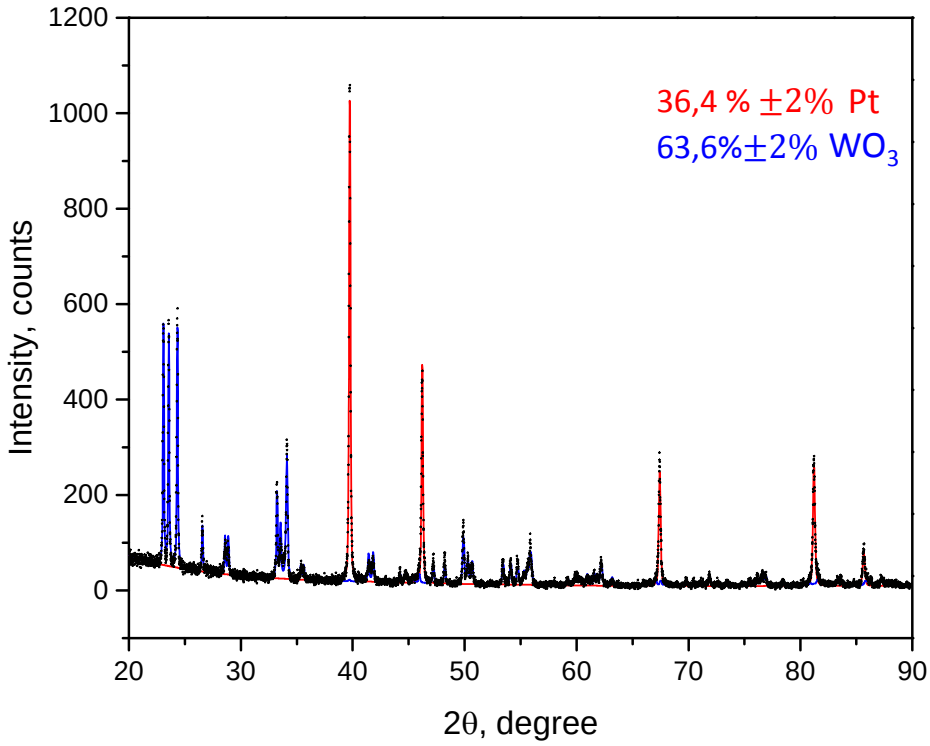

Fig. S8. XRD pattern of the PtW_{mod}/C sample after thermo-oxidation at 1000^0C in Ar+21%O_2 atmosphere.

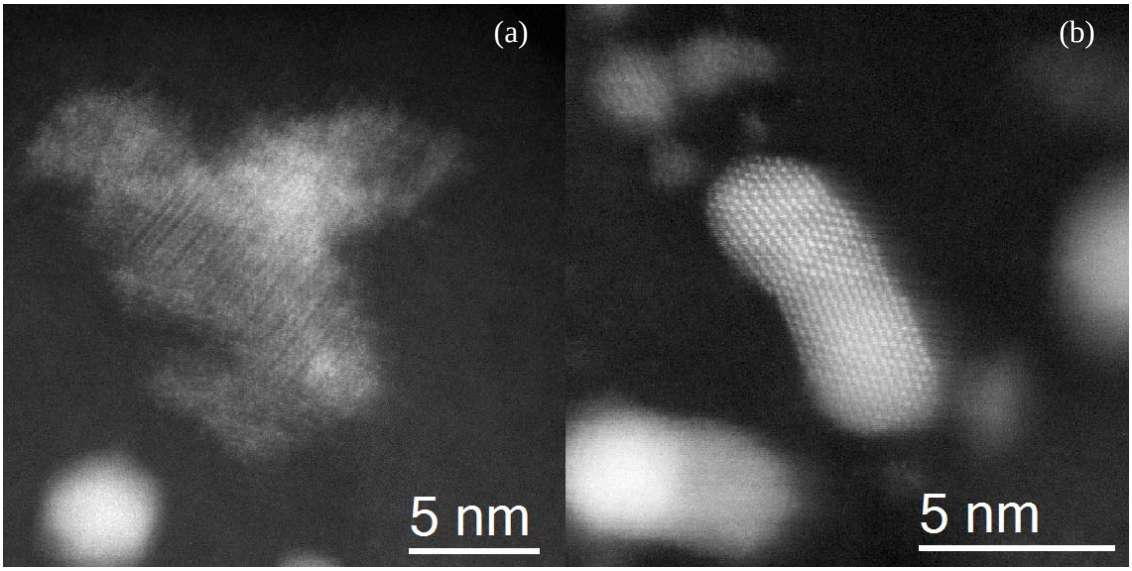

Fig. S9. HAADF STEM micrographs demonstrating an ordering of the WOx amorphous clusters.

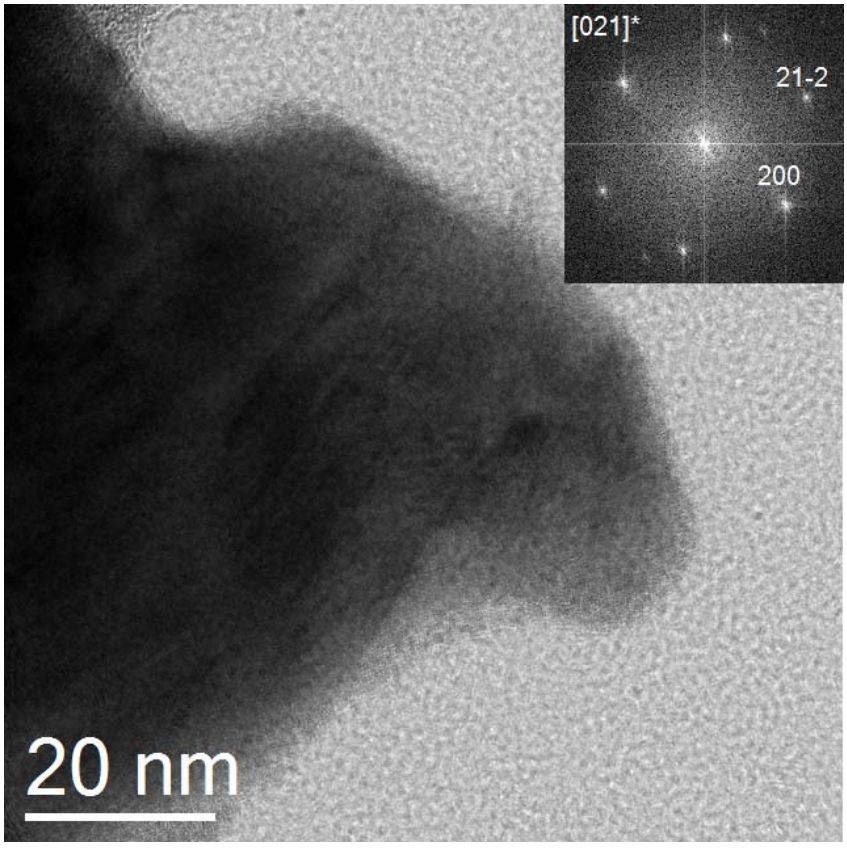

Fig. S10. HRTEM micrograph of the PtW_{mod}/C sample after electrochemical corrosion test. The corresponding FFT pattern (inset) shows a single crystalline diffraction due to the WO_2 phase.